Appl. Phys. B 40, 133–139 (1986)

Applied Physics B Photophysics and Laser Chemistry

Collective Modes – An Analytical Model for Active Mode Locking in the Transient Case

P. Aechtner and A. Laubereau

Physikalisches Institut, Universität, D-8580 Bayreuth, Fed. Rep. Germany

Received 1 April 1986/Accepted 15 April 1986

Abstract. A novel concept is presented for the pulse generation in the linear regime of an actively loss modulated laser. Introducing collective laser modes, the frequency detuning of the modulator and the statistical initial situation of the laser starting from spontaneous emission become tractable. Formation of a mode-locked pulse is described by the selection of collective modes. Perfect mode locking corresponds to the survival of a single mode in the build-up process. A variety of laser properties is derived from the solution and compared with experiment. The model predicts imperfect mode locking (with a finite number of collective modes) in the transient case in agreement with experimental findings.

PACS: 42.55 Bi, 42.60 He

The demand for short and reproducible pulses has renewed the interest in understanding active mode locking (AM) of pulsed laser systems. It has been shown, for example, that this operation mode combined with passive mode locking increases the reproducibility of short and intense pulses [1–4]. Actively mode locked and Q-switched oscillators are also considered as a stable and reliable pulse source for laser-fusion systems [5–7].

The theory of stationary mode locking applicable to cw lasers is well established [8–10]. For the transient conditions of pulsed lasers, however, the theoretical treatment is still subject to discussion. For the analytical description of this situation a very simple model has been recently proposed assuming a special initial condition for the mode locking process [11]. The laser action is considered to start at $t=0$ with a single axial mode while neighbouring additional modes are subsequently excited under the effect of the active mode locker. The statistical character of the initial condition of multi-mode lasers starting from spontaneous emission is not contained in this picture [12]. In fact, comparing theory and experiment, deviations from theoretical predictions have been noted and attributed to this point [6].

In this paper an alternative approach is presented which incorporates the complicated temporal and frequency structure of the initial spontaneous fluorescence. Introducing the concept of collective modes replacing the longitudinal frequency cavity modes, analytical solutions for the build-up of laser radiation in the linear regime are derived in closed form. Our results will be compared with previous work and with experimental data on a pulsed Nd:glass laser oscillator.

1. Theoretical Model

The physical situation is illustrated by Fig. 1. The laser system is schematically shown in Fig. 1a. It consists of the optical cavity, the active medium for light amplification and the acousto-optic mode locker for active loss modulation. The specific kind of optical resonator used is not relevant for the following discussion which applies for Fabry-Perot and ring cavities. The transmission η of the active mode locker is depicted in Fig. 1b; it varies periodically in time according to:

$$\eta(t)=\eta_0+\eta_1\cos\Omega' t \tag{1}$$

with average value η_0, modulation amplitude η_1, and frequency Ω'. The maximum transmission is usually close to 1, $\eta_{max}=\eta_0+\eta_1\simeq 1$. Higher harmonics are neglected by (1) which is a good approximation for

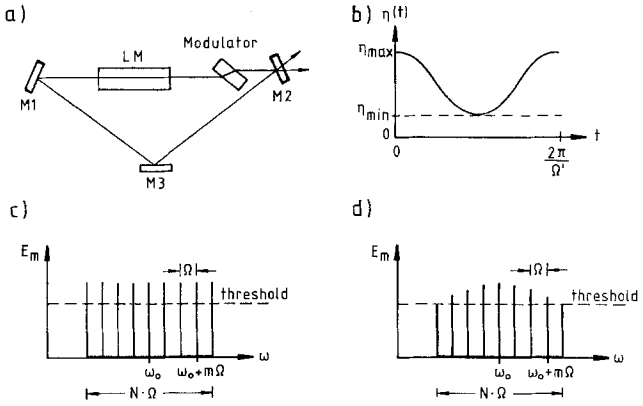

Fig. 1. (a) Schematic of actively mode locked laser oscillator; mirrors M_1–M_3, laser medium LM; (b) transmission $\eta(t)$ of the active mode locker versus time; modulation frequency Ω'; (c) and (d) spectrum of amplified cavity modes for a rectangular gain profile (c) and for a parabolic gain profile (d); the shown frequency dependence is exaggerated; center of gain profile ω_0; frequency spacing of cavity modes Ω

many experimental systems. The spectral properties of the laser medium are depicted in Figs. 1c and d. In the first part of this paper, a rectangular gain profile of the active medium is assumed which allows N equally spaced longitudinal cavity modes to be amplified (Fig. 1c). The more general case of a parabolic gain profile with N longitudinal modes above threshold is subsequently discussed (Fig. 1d). The frequency spacing of the modes is given by

$$\Omega = 2\pi c/L \tag{2}$$

(with cavity length L). Ω may differ by a certain frequency mismatch

$$\Delta\omega = \Omega - \Omega' \tag{3}$$

from the modulation frequency. It is obvious from Fig. 1c that the longitudinal modes form a set of equal oscillators of constant spacing in frequency domain. The analogy to the well-known linear chain in solid state physics suggests a collective mode picture for the analytic treatment of the mode locked laser.

The total electromagnetic field in the cavity is obtained by a superposition of the set of longitudinal modes

$$E(t) = \exp(\mathrm{i}\omega_0 t) \sum_{m=-(N-1)/2}^{m=(N-1)/2} A_m(t) \times \exp[\mathrm{i}m\Omega t + \mathrm{i}\phi_m(t)], \tag{4}$$

where A_m and ϕ_m, respectively, denote the amplitude and phase of the m-th cavity mode. ω_0 marks the center of the gain profile (N uneven). As discussed in [13] the build-up of the laser emission from spontaneous emission is represented by a random distribution of initial phases ϕ_m.

1.1. Rectangular Gain Profile

For tutorial reasons we consider the case of a flat gain profile which is switched on at $t=0$ and provides constant amplification. With respect to the linear cavity losses (except the mode locker) we introduce the net gain $K>1$ per cavity pass and see immediately that

$$E(t+T) - E(t) = [K\eta(t) - 1]E(t); \tag{5}$$

$T=L/c$ denotes the cavity round trip time. Substituting (4) into (5) and equating terms with same frequency $\omega_0 + m\Omega$ we arrive at

$$\begin{aligned} \Delta E_m &= E_m(t+T) - E_m(t) \\ &= (K\eta_0 - 1)E_m + \frac{K\eta_1}{2} E_{m+1} \exp(\mathrm{i}\Delta\omega t) \\ &\quad + \frac{K\eta_1}{2} E_{m-1} \exp(-\mathrm{i}\Delta\omega t). \end{aligned} \tag{6}$$

Here $E_m(t) = A_m(t)\exp(\mathrm{i}\phi_m)$ is the complex field amplitude of the m-th cavity mode.

The build-up of the laser radiation requires a large number of round trips; i.e. the mode amplitude E_m changes slowly for small net gain K. It is therefore convenient to convert the difference equations (6) to differential equations

$$\begin{aligned} \frac{dE_m}{dt} &= \alpha E_m + \frac{\beta}{2} E_{m+1} \exp(\mathrm{i}\Delta\omega t) \\ &\quad + \frac{\beta}{2} E_{m-1} \exp(-\mathrm{i}\Delta\omega t) \end{aligned} \tag{7}$$

with $\alpha = (K\eta_0 - 1)/T$ and $\beta = K\eta_1/T$. Equation (7) readily shows that modes $(m+1)$ and $(m-1)$ effect the time evolution of the m-th mode via the modulation parameter β. The direct analogy of this expression for the resonant case ($\Delta\omega = 0$) with the well-known equation of motion of a one-dimensional monatomic lattice should be noted.

Following this analogy, we introduce the periodic boundary condition

$$E_m(t) = E_{m+N}(t) \tag{8}$$

which holds for sufficiently large N. We recall that $N \sim 10^3$ for mode locked solid state lasers and even larger for dye lasers. Use of (8) implies that the accurate evaluation of the mode amplitudes close to the boundary $m = \pm(N-1)/2$ is not important because of the little effect these modes have on the total field E.

We are looking for solutions in terms of a Fourier series

$$E_m = \sum_l B_l \exp(-\mathrm{i}m\Omega\tau_l) \tag{9}$$

with (weakly) time dependent expansion coefficients $B_l(t)$. Application of the boundary condition (8) gives

$$\tau_l = T\frac{l}{N}; \quad l=0, \pm 1 \ldots \pm \frac{N-1}{2}. \tag{10}$$

Inserting (9) in (7) leads to the solution

$$B_l(t) = B_{l0} \times V_l(t), \tag{11}$$

where we introduce here the amplification factor of the l-th collective mode

$$V_l(t) = \exp\left\{\alpha t + \frac{\beta}{\Delta\omega}[\sin(\Delta\omega t - \Omega\tau_l) + \sin\Omega\tau_l]\right\}. \tag{12}$$

The initial values B_{l0} at $t=0$ have to be determined from the spontaneous emission at the beginning of the lasing process.

Combining (4, 9, 11, 12) the summation over the longitudinal modes can be carried out yielding the total laser field

$$E(t) = \sum_{l=-(N-1)/2}^{(N-1)/2} \tilde{E}_l(t), \tag{13}$$

where

$$\tilde{E}_l(t) = B_{l0} V_l(t) \frac{\sin[N\Omega(t-\tau_l)/2]}{\sin[\Omega(t-\tau_l)/2]} \exp(i\omega_0 t). \tag{14}$$

The temporal shape of the field component $\tilde{E}_l$ is the Fourier transform of the rectangular gain profile under consideration. τ_l states the temporal position of $\tilde{E}_l$ in the cavity. According to (14) the component $\tilde{E}_l$ represents a pulse which is inherent to the laser field. The $\tilde{E}_l$'s will be termed collective modes in the following.

The starting point of the amplification process is provided by spontaneous emission. In our model, the mean intensity at $t=0$ is given by

$$I_0 = \frac{c}{8\pi}|E(0)|^2_{av} = \frac{c}{8\pi}\left|\sum_l \tilde{E}_l(0)\right|^2. \tag{15}$$

The subscript "av" indicates the average over the cavity transit time, $-T/2 \leqq t \leqq T/2$. Values of $I_0 \sim 10^{-4}$ W/cm^2 may be estimated as equivalent noise input for the Nd : glass laser [14].

Writing $B_{l0} = |B_{l0}| \exp(i\Phi_l)$ we introduce the phase factors Φ_l of the collective modes, the statistical nature of which should be noted. Evaluating the r.h.s. of (15) we neglect the sum over cross terms because of the random phases Φ_l and obtain

$$\sum_l |B_{l0}|^2 \simeq \frac{8\pi}{c}\frac{I_0}{N}. \tag{16}$$

Equation (16) represents a normalizing condition for the initial amplitudes B_{l0}.

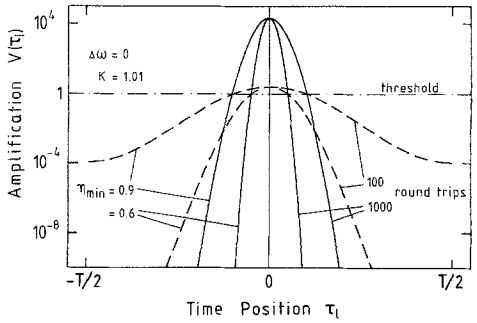

Fig. 2. Amplification $V(\tau_l)$ versus time position τ_l of the collective modes after 100 and 1000 cavity round trips (broken and solid curves, respectively); $\eta_{min} = 0.9$ and 0.6, $\eta_{max} = 1$; cavity round trip time T

Selection of Collective Modes. The analytic result of (12–14) predicts that the amplification $V_l(t)$ is different for the various modes l. The formation of a mode locked laser pulse is described by this l-dependence. An example is presented in Fig. 2 for a certain number of cavity round trips ($t = \text{const}$). The resonant case $\Delta\omega = 0$ is considered where

$$V_l = V(\tau_l) = \exp(\alpha t + \beta t \cos\Omega\tau_l). \tag{17}$$

A small net amplification of $K=1.01$ and two different values for the mode locker efficiency, $\eta_{min} = 0.9$ and 0.6, are assumed ($\eta_{max} = 1$). The amplification $V(\tau_l)$ is plotted in Fig. 2 versus the temporal position τ_l of the collective modes. $\tau_l = 0$ marks the position with maximum transmission $\eta_{max} = \eta_0 + \eta_1$ of the mode locker while the modes at $\tau_l = \pm T/2$ meet the minimum transmission $\eta_{min} = \eta_0 - \eta_1$. At $t=0$ the amplification is completely flat, $V(\tau_l) = 1$ (see dash-dotted line), while highly interesting features develop after 100 and 1000 cavity round trips (broken and solid curves in Fig. 2, respectively). Only the central part of collective modes finds positive gain while field components with infavourable position τ_l remain below threshold. In this way the effective number of amplified modes significantly decreases with increasing number of cavity transits. The selection process is favoured by a larger efficiency of the mode locker (smaller η_{min}).

1.2. Parabolic Gain Profile

Light amplification in the laser depends on frequency. For many cases, an expansion around the gain maximum at ω_0 to second order will be valid leading to a parabolic profile

$$K(\omega) = K_0 - K_1(\omega - \omega_0)^2. \tag{18}$$

K_1 is a measure of the width of the net gain profile. Equation (7) for the amplitudes of the longitudinal

modes now reads

$$\frac{dE_m}{dt} = \alpha(m)E_m + \tfrac{1}{2}\beta(m+1)\exp(\mathrm{i}\Delta\omega t)E_{m+1} + \tfrac{1}{2}\beta(m-1)\exp(-\mathrm{i}\Delta\omega t)E_{m-1}, \quad (19)$$

where the parameters α, β have the form

$$\alpha(m) = \alpha_0 - \alpha_1 m^2, \qquad \beta(m) = \beta_0 - \beta_1 m^2. \quad (20a)$$

The peak values are denoted by $\alpha_0 = (K_0\eta_0 - 1)/T$ and $\beta_0 = K_0\eta_1/T$. The frequency dependence of the gain curve is expressed by the coefficients

$$\alpha_1 = K_1\eta_0\Omega^2/T; \quad \beta_1 = K_1\eta_1\Omega^2/T. \quad (20b)$$

The number of longitudinal modes E_m above threshold is given by (Fig. 1d)

$$N \simeq 2\left(\frac{\alpha_0+\beta_0}{\alpha_1+\beta_1}\right)^{1/2}. \quad (21)$$

For an approximate solution we make a Fourier ansatz similar to (9)

$$E_m(t) = \sum_l B_l(t)\exp[-(\alpha_1+\beta_1)tm^2 - \mathrm{i}m\Omega\tau_l(t)], \quad (22)$$

where $|l| \leqq (N-1)/2$ and the mode position τ_l is allowed to drift slowly during the lasing process; $\tau_l(0)$ is given by (10). Since the laser radiation has to be synchronized with the mode locker (selection of time modes) we restrict the discussion to the case $|\Omega\tau_l| \ll 1$ and small frequency detuning, $|\Delta\omega t| \ll 1$. For these approximations and for small net gain per cavity round trip $[K_0(\eta_0+\eta_1)-1 \ll 1]$ our ansatz (22) solves (19); we yield after some algebraic manipulation

$$B_l(t) = B_{l0} \times V_l(t), \quad (23a)$$

$$V_l(t) \simeq \exp\left\{\alpha_0 t + \frac{\beta_0}{\Delta\omega}[\sin(\Delta\omega t - \Omega\tau_l) + \sin\Omega\tau_l]\right\}, \quad (23b)$$

and

$$\tau_l(t) \simeq \tau_l(0)[1 - \beta_0(\alpha_1+\beta_1)t^2] - \frac{2\Delta\omega}{3\Omega}\beta_0(\alpha_1+\beta_1)t^3. \quad (23c)$$

For the validity range of the approximation, the result for V_l is the same as for the rectangular gain profile, compare (12).

Inserting (22 and 23) into (4) we reproduce (13) and find

$$\tilde{E}_l(t) \simeq B_{l0}V_l(t)\left(\frac{\pi}{(\alpha_1+\beta_1)t_M}\right)^{1/2} \times \exp[-(t-t_M-\tau_l)^2/t_c^2 + \mathrm{i}\omega_0 t]; \quad (24)$$

$t_M = MT$ denotes the time required for M cavity round trips ($M \gg 1$). As a consequence of the parabolic gain profile, the collective modes have Gaussian shape with 1/e duration

$$t_c = 2[(\alpha_1+\beta_1)t_M]^{1/2}/\Omega. \quad (25)$$

It is interesting to see that t_c slowly increases with the number of round trips. This effect corresponds to the well-known spectral narrowing of the amplification process.

2. Discussion

Comparing (23) and (11, 13) we note that the mechanism for selecting l-modes in the amplification process is very similar for rectangular or parabolic gain profile. Different modes starting from statistical initial amplitudes B_{l0} find different gain V_l depending on the temporal position τ_l with respect to the mode locker. Figure 3 illustrates this point. Using (12–15) the intensity $|E(t)|^2$ of the laser emission has been computed for $N = 10^3$ longitudinal modes. At $t = 0$, 10^3 fluctuations due to spontaneous emission are contained in the cavity and extend over the whole round trip time T (not shown in Fig. 3). After 500 round trips the radiation has been amplified by a factor of 2×10^4 but only ~ 28 collective modes in a small interval $|\tau_l| \lesssim 1.5 \times 10^{-2}\, T$ have survived (Fig. 3a). The result for 1300 round trips with amplification $\sim 2 \times 10^{11}$ is shown in Fig. 3b. A smaller number of ~ 17 spikes has survived which are positioned at $|\tau_l| \lesssim 1 \times 10^{-2}\, T$.

Ideal mode locking in this picture corresponds to the survival of a single collective mode at $\tau_l = 0$. The build-up time t_{ml} for perfect mode locking may be estimated from (23 and 25). We define t_{ml} as the necessary time for the amplification V_0 of the central

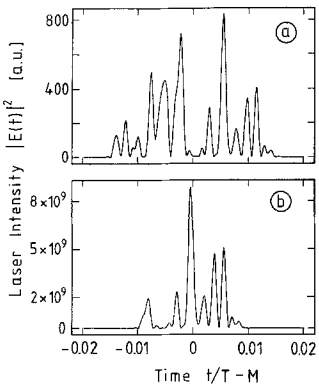

Fig. 3a and b. Intensity of the laser emission versus time for $N = 1000$ longitudinal cavity modes and a rectangular gain profile; $K = 1.01$; $\eta_{\min} = 0.3$; $\Delta\omega = 0$; (a) after $M = 500$ round trips; (b) after $M = 1300$ round trips. The intensity spikes represent the collective modes l introduced theoretically; the strong selection of collective modes due to the active mode locker should be noted

mode to exceed the gain V_l of modes at $\tau_l = t_c$ by a factor of e. For the resonant case ($\Delta\omega = 0$) we find

$$t_{ml} = [2\beta_0(\alpha_1 + \beta_1)]^{-1/2} \simeq NT[8\eta_1 K_0(K_0 - 1)]^{-1/2}. \tag{26}$$

Equation (26) allows an estimate of the duration of the transient mode locking region, i.e. the time required to reach stationary conditions for a homogeneously broadened laser line where gain depletion does not effect α_1 and β_1. Setting $K_0 = 1.01$, $\eta_1 = 0.25$, and $T \simeq 10^{-8}$ s we estimate the build-up time for the Nd : glass laser [$N \simeq 7 \times 10^3$, see (21)] to be $t_{ml} \sim 0.5$ ms. The cw Nd : YAG system ($N \simeq 500$) is characterized by $t_{ml} \simeq 30$ µs, which agrees with published data [6, 11].

The pulse duration of the laser emission is governed by two processes: shortening due to selection of modes $\tilde{E}_l$ and lengthening of the individual mode because of spectral gain narrowing, see (23 and 25), respectively. At $t \simeq t_{ml}$ the minimum duration t_{p0} is produced which characterizes the steady state pulse. Denoting by t_{p0} the halfwidth of the laser intensity (FWHH) we obtain from (25)

$$t_{p0} = \frac{\sqrt{8\ln 2}}{\Omega}\left(\frac{\alpha_1 + \beta_1}{2\beta_0}\right)^{1/4}. \tag{27}$$

Equation (27) predicts similar values as the steady state theory of Kuizenga et al. [8]. For $T \simeq 10^{-8}$ s and $\eta_1 = 0.25$, a reasonable value of 90 ps is estimated for the cw Nd : YAG laser.

Experimental conditions must be stable over t_{ml} to approach steady state. In particular the synchronization between the active mode locker and the propagating collective modes in the cavity has to be maintained; i.e. the tolerable detuning $\Delta\omega_0$ has to be sufficiently small. From (23) we realize that $\Delta\omega_0 t \lesssim \Omega\tau_l$ in order to select the mode $l = 0$. Setting $t \simeq t_{ml}$ and $\tau_l \simeq t_{p0}/2$ for the position of the competing modes we arrive at

$$\Delta\omega_0 \simeq \sqrt{2\ln 2}[2\beta_0(\alpha_1 + \beta_1)^3]^{1/4}. \tag{28}$$

For the cw YAG-laser ($T = 10^{-8}$ s, $\eta_1 = 0.25$) we estimate a value of $\simeq 200$ Hz for perfect mode locking with minimum duration t_{p0}.

In the transient region $t < t_{ml}$ imperfect mode locking can be achieved, only. In these cases the active mode locker acts as an effective time gate for the sequence of amplified collective modes. Taking the full width t_p at half maximum of the amplification profile $V(\tau_l)^2$ as a measure of the duration of the laser emission we find from (13) for the rectangular gain profile

$$t_p \simeq \frac{T}{\pi}\arccos\left(1 - \frac{\Delta\omega \ln 2}{4\beta \sin(\Delta\omega t_M/2)}\right); \tag{29}$$

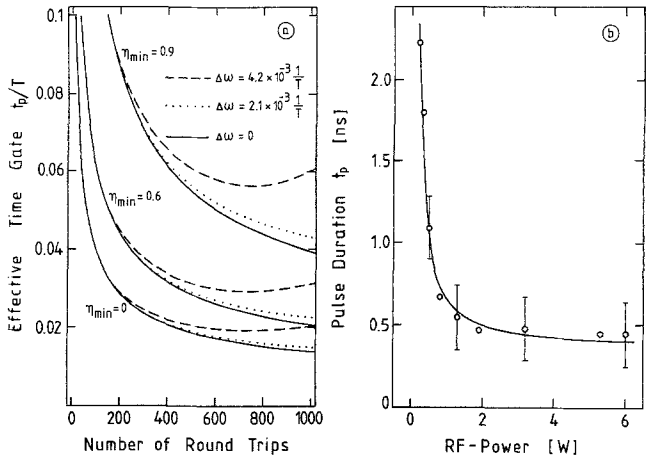

Fig. 4. (a) Effective time gate t_p/T of the amplification profile versus number of round trips for different modulator efficiencies $\eta_{min} = 0.9$, 0.6, and 0; $K = 1.01$. Three values of frequency detuning $\Delta\omega \times T = 0$, 2.1×10^{-3} and 4.2×10^{-3} are considered (solid, dotted, and broken curves, respectively). (b) Measured pulse duration t_p versus input RF power of the mode locker for a Nd : glass laser with Fabry-Perot cavity

t_p depends on t_M, i.e. number of round trips of the amplification process. At resonance, $\Delta\omega = 0$, (29) yields

$$t_p \simeq \frac{T}{\pi}\left(\frac{\ln 2}{\beta t_M}\right)^{1/2}. \tag{29a}$$

This result also holds for the parabolic gain profile. t_p decreases with increasing mode locker efficiency (parameter β) and amplification time. The result of (29a) is similar to earlier findings [11], but predicts longer pulses by a factor of $\simeq\sqrt{8}$. We note that the statistical character of the initial condition has (partially) survived, i.e. a substructed pulse of duration t_p is generated (Fig. 3).

Some numerical results on the duration of the laser emission are presented in Fig. 4a. A net intensity amplification of 2% per round trip ($K = 1.01$) and three mode locker efficiencies with minimum transmission $\eta_{min} = 0.9$, 0.6, and 0 ($\eta_{max} = 1$) are considered. The duration t_p/T is plotted versus number of round trips, t_M/T for three values of frequency tuning $\Delta\omega = 0$ (solid curves), $\Delta\omega = 2.1 \times 10^{-3}/T$ (dotted lines) and $\Delta\omega = 4.2 \times 10^{-3}/T$ (broken curves), respectively. t_p first shortens with increasing number of round trips depending on the modulator efficiency and frequency detuning. For $\Delta\omega = 4.2 \times 10^{-3}/T$, the shortening terminates after ~ 750 round trips because of the large phase shift (180°) which has built up between the mode locker and the propagating pulses in the cavity (broken curves in Fig. 4a). For frequency matching $\Delta\omega = 0$ the synchronization of the mode locker is maintained and the shortening process continues. The minimum value

for t_p after 1000 round trips is $t_p \simeq 0.014\,T$ (solid curve for $\eta_{\min}=0$).

We note that the frequency matching requirements are relaxed in the transient case in comparison with stationary conditions. Following the same arguments as used above in context with (28) we estimate the tolerable mismatch $\Delta\omega$ to be

$$\Delta\omega = \Delta\omega_0 \times \frac{t_{ml}}{t_M} \times \frac{t_p}{t_{p0}}. \tag{30}$$

It is interesting to compare t_p with the bandwidth of the laser. From gain narrowing arguments the spectral width $\delta\nu_L$ (FWHH) of the laser emission is evaluated to be

$$\delta\nu_L = \frac{1}{T}\left(\frac{2\ln 2}{(\alpha_1+\beta_1)t_M}\right)^{1/2}. \tag{31}$$

This leads to the product

$$t_p \times \delta\nu_L = \frac{\ln 2}{\pi t_M}[\beta_0(\alpha_1+\beta_1)/2]^{-1/2}. \tag{32}$$

The laser emission is not transform limited ($t_M < t_{ml}$). Only, when the laser approaches the stationary regime ($t_M \to t_{ml}$) one finds $t_p \to t_{p0}$ and $t_p \times \delta\nu_L \to 2\ln 2/\pi$ as required for an ideal Gaussian pulse.

3. Comparison with Experiment

Some features of the active mode locking under transient condition have been demonstrated experimentally investigating a pulsed Nd:glass laser. The pulse duration of the mode-locked radiation was measured using the conventional intensity autocorrelation technique with a nonlinear crystal (KDP) and/or a fast photodiode with a transient digitizer with ~ 1 ns time resolution. Duration of the flash lamp pulse pumping the laser rod is 300 µs. Some results of the effect of the modulator efficiency on the pulse duration are presented in Fig. 4b. t_p is plotted versus the input power P_{RF} of the modelocker. Assuming $\eta_1 \propto P_{RF}^{1/2}$, (29a) predicts $t_p \propto P_{RF}^{-1/4}$ [11]. The experimental curve (solid line) in Fig. 4b is in qualitative agreement with this relationship yielding $t_p \simeq 450$ ps for a RF power of several watts.

It is important to compare the pulse duration with the spectral width of the laser emission. Our experimental result of $\delta\nu_L/c = 5 \pm 1\ \mathrm{cm}^{-1}$ indicates a large product $t_p \times \delta\nu_L \simeq 70$ for $t_p = 450$ ps far above the Fourier limitation. Only imperfect mode locking is achieved as expected from our theoretical model.

Equation (13) presents an analytical result for the amplification process which can be tested by the threshold behaviour of the laser. The threshold is found experimentally detecting the laser emission at a certain intensity level necessary for the measuring system. A constant total amplification V_{thr} is required to reach the detection threshold. From (12) we find maximum gain for time modes with $\Omega\tau_l = -\Delta\omega t_M/2$ and derive

$$K_{thr}(\Delta\omega) = \frac{1+\dfrac{T}{t_M}\ln V_{thr}}{\eta_0 + 2\eta_1 \sin(\Delta\omega t_M/2)/\Delta\omega t_M}. \tag{33}$$

K_{thr} represents the necessary single pass gain at laser threshold. This quantity may be also expressed in terms of the mirror reflectivities R_1, R_2, the amplification of the laser material $\exp(G_{thr})$ and additional cavity losses represented by a factor T_0

$$K_{thr} = R_1 R_2 T_0 \exp(G_{thr}). \tag{34}$$

Assuming a quadratic dependence of the laser amplification on the pump voltage U of the flash lamp, $G_{thr} = (U_{thr}/U_0)^2$, we arrive at

$$U_{thr}(\Delta\omega) = U_0\left(\ln\frac{K_{thr}(\Delta\omega)}{R_1 R_2 T_0}\right)^{1/2}. \tag{35}$$

U_0 denotes a scaling factor of the pumping process which can be determined varying the linear losses T_0 of the cavity. We are now in the position to compare (33 and 35) with experimental data. Results are shown in Fig. 5. It is convenient to keep the mode locker frequency constant and vary the cavity length. We therefore introduce the length mismatch ΔL of the (full) round trip length L

$$\Delta L = -\frac{L^2}{2\pi c}\Delta\omega \tag{36}$$

($\Delta L \ll L$). V_{thr} is plotted in the figure in units of V_{thr} ($\Delta L = 0$) versus ΔL. A value of $L = 3.0$ m and two mode

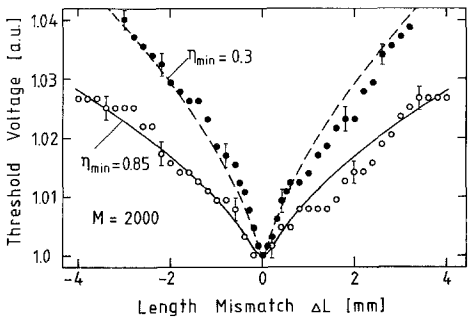

Fig. 5. Threshold voltage versus length mismatch for a pulsed Nd:glass laser with Fabry-Perot cavity and two modulator efficiencies ($\eta_{min} = 0.85$ and 0.3, respectively; $\eta_{max} = 1$); experimental points, calculated curves. A threshold minimum is predicted in agreement with experimental findings

locker efficiencies, $\eta_{\min}=0.85$ (open circles) and $\eta_{\min}=0.3$ (full points) are experimentally adjusted.

Changing the cavity length over several mm a variation of the threshold voltage of a few per cent is observed. The curves in Fig. 5 are calculated from (33–36). The only fitting parameter in the calculation is the number of round trips, $M=t_M/T$ while the other parameters are known from independent measurements. $V_{\text{thr}}\simeq 10^5$ is estimated from spontaneous fluorescence and the detected threshold level of $\simeq 10^6$ W/cm^2; the precise value is of minor importance for U_{thr}. It is interesting to see that the calculated curves account well for the experimental points for $M=2000$. The minimum of the threshold curve has practical importance to adjust the resonance case, $\Delta L=0$ [1].

4. Conclusions

In summary we point out that an analytical model has been derived for active mode locking in the transient case in the absence of nonlinear effects. Our theoretical derivation accounts for the statistical initial condition of the laser emission starting from spontaneous fluorescence. Salient features of the model agree with experimental findings. In particular, imperfect mode locking is predicted and experimentally observed in the transient case, in contrast to conclusions from a different treatment reported recently [11]. Our model also yields reasonable estimates for the stationary case.

The analytical description is based on collective modes of the laser field instead of the conventional frequency modes. A mode selection mechanism during the build-up of laser radiation strongly reduces the effective number of collective modes by a factor of 10^2 to 10^3. The corresponding simplification of numerical computations makes the collective mode picture also highly valuable for a nonlinear stage of the lasing process where additional effects, e.g. nonlinear absorption of a passive mode locker or gain depletion of the laser material, have to be taken into account.

References

1. H.P. Kortz, IEEE J. Quant. Electron. QE-19, 578 (1983).
2. G.P. Albrecht, J. Bunkenburg, Opt. Commun. **38**, 377 (1981).
3. M.A. Lewis, J.T. Knudtson, Appl. Optics **21**, 2897 (1982).
4. L.S. Goldberg, P.E. Schoen, IEEE J. Quant. Electron. QE-20, 628 (1984).
5. D.J. Kuizenga, IEEE J. Quant. Electron. QE-17, 1694 (1981).
6. G.F. Albrecht, M.T. Gruneisen, D. Smith, IEEE J. Quant. Electron. QE-21, 1189 (1985).
7. E.W. Roschger, A.P. Schwarzenbach, J.E. Balmer, H.P. Weber, IEEE J. Quant. Electron. QE-21, 465 (1985).
8. D.J. Kuizenga, A.E. Siegman, IEEE J. Quant. Electron. QE-6, 694 (1970).
9. D.J. Kuizenga, A.E. Siegman, IEEE J. Quant. Electron. QE-6, 709 (1970).
10. A.E. Siegman, D.J. Kuizenga, Opto-Electron. **6**, 43 (1974).
11. D.J. Kuizenga, D.W. Phillion, T. Lund, A.E. Siegman, Opt. Commun. **9**, 221 (1973).
12. C.C. Wang, L.I. Davis, Jr., Appl. Phys. Lett. **19**, 167 (1971).
13. P.G. Kryukov, V.S. Letokhov, IEEE J. Quant. Electron. QE-8, 766 (1972).
14. B. Hausherr and H. Weber, Z. Ang. Math. Phys. **22**, 1155 (1971).